

ELECTRICAL SIMULATION OF THE CIRCULATORY SYSTEM*

A. K. Tsaturyan

UDC 611.08:539

An electrical model of the arterial part of the human vascular system is proposed. This model is used to investigate the impedance, the shape of the pressure and flow waves, and the static characteristics of the vascular system under normal conditions and in the case of artificial circulation. In order to simulate the ACA pump, the problem of the quasi-one-dimensional flow of a viscous fluid in a tube with wave-type variation of the radius is considered. A comparison of the results with the results of direct measurements in man shows that they are in qualitative and quantitative agreement. Simulation also reveals certain characteristics of pulse-wave propagation in artificial circulation. An explanation of the effects observed is proposed, and their possible influence on the activity of the organism is discussed.

§ 1. Model Equations

In modeling segments of the arteries we used the analogy between the electrical processes in a long cable and the quasi-one-dimensional equations of motion of a viscous fluid in an elastic tube. In deriving the telegraph equations from the Navier-Stokes equations and the equations of shell theory it is necessary to make a series of assumptions, such as the assumption that the flow is axisymmetric and the radius of the vessel small as compared with the length of the pulse wave, etc. The validity of these assumptions was discussed in [1], where it is also possible to find a derivation of the telegraph equations from the equations of mechanics. The blood flow in an arterial segment has been described by the system

$$\frac{\rho}{F} \frac{\partial g}{\partial t} + \frac{8\pi\mu}{F^2} g + \frac{\partial p}{\partial x} = 0; \quad \frac{\partial g}{\partial x} + \frac{\partial F}{\partial t} = 0; \quad \frac{\partial F}{\partial t} = \frac{3r_w F}{2Eh} \frac{\partial p}{\partial t}, \quad (1)$$

where g , p , ρ , μ , F , r_w , h , E are the flow rate, pressure, density, and viscosity of the blood, the cross-sectional area and radius of the vessel, and the thickness and Young's modulus of the vessel wall, respectively; z and t are the axial coordinate and time. In order further to simplify Eqs. (1), we replace the partial derivatives with respect to x by the finite differences of the values at the ends of the segment:

$$\frac{\rho l}{F} \dot{g}(t) + \frac{8\pi\mu l}{F^2} g(t) + p(t) - p_0(t) = 0; \quad g(t) - g_0(t) + \frac{3Fr_w l}{2Eh} p(t) = 0. \quad (2)$$

Here g_0 and p_0 are the flow rate and pressure in the inlet section; g and p are the same variables at the segment outlet. The order of approximation of system (1) by system (2) is equal to l/λ , where l is the length of the segment and λ is the pulse-wavelength. Clearly, even for segments several tens of centimeters long, the accuracy of approximation is good enough, and, consequently, the construction of models containing hundreds of short segments is not always justified. In order to describe organic circulation, we used the equation $RC\dot{p}_0(t) + p_0(t) - p_V = RCR_0g_0(t) + (R + R_0)\dot{g}_0(t)$, where p_V is the venous pressure, which is assumed constant; C is the elasticity of the vascular system of the organ; R_0 is the resistance of the small arteries; R is the resistance of the arterioles, capillaries, and venules. In order to describe the flow of

*Paper presented at the First All-Union Conference on Engineering and Medical Biomechanics, Riga, October, 1975.

M. V. Lomonosov Moscow State University. Translated from *Mekhanika Polimerov*, No. 4, pp. 761-765, July-August, 1975. Original article submitted January 21, 1975.

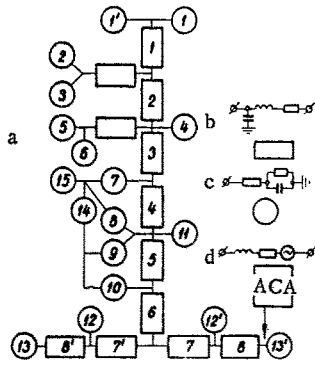


Fig. 1

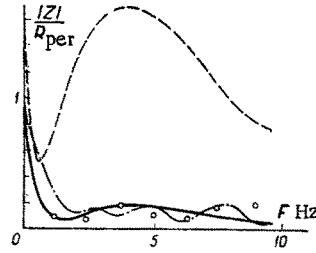


Fig. 2

Fig. 1. Block diagram of model (a), basic circuits of arterial segment (b; notation same as in Table 2), peripheral segment (c; notation same as in Table 3), and ACA analog (d).

Fig. 2. Frequency dependence of absolute value of dimensionless impedance. (—) model in regime A; (---) model in regime B; (-·-·-) model of [3]; (○) measurements in man [4]. Total peripheral resistance in regime A — $R_{per} = 1.4 \cdot 10^8 \text{ kgf} \cdot \text{m}^{-4} \cdot \text{sec}^{-1}$.

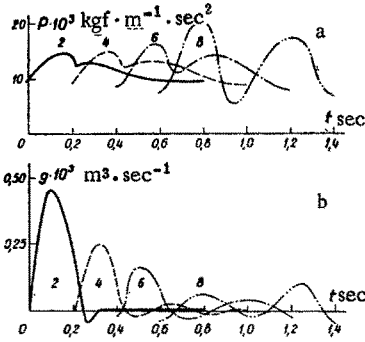


Fig. 3. Pressure- (a) and flow- (b) wave amplitudes measured on the model in regime B in arterial segments 2, 4, 6, and 8.

blood in the roller-type ACA pump we used the first two equations of system (1), F being assumed to be a given function of x and t :

$$F(x, t) = F_0 \left[1 + \tau \cos \frac{2\pi}{\Delta} (vt - x) \right]; \quad (3)$$

τ , Δ , and v are the compression factor, the length of the working section of the pump, and the roller speed. Substituting (3) in the second equation of system (1) and integrating, we obtain

$$g(x, t) = \int_0^x - \frac{\partial F(\eta, t)}{\partial t} d\eta + g(0, t); \quad (4)$$

$$g(0, t) = g(\Delta, t) = g_0(t).$$

We now substitute (4) in the first equation of (1) and integrate with respect to x from 0 to Δ . After certain manipulations, we obtain the final equation of the pump:

$$\rho \Delta F_0^{-1} (1 - \tau^2)^{-1/2} \dot{g}_0(t) + 8\pi\mu \Delta F_0^{-2} (1 - \tau^2)^{-3/2} g_0(t) + p(t) - p_0(t) =$$

$$= 8\pi\Delta\mu\tau^2 F_0^{-1} (1 - \tau^2)^{-1/2} + 2\pi v \tau (1 - \tau^2)^{-1/2} \{ \rho^2 v^2 + [4\Delta\mu F_0^{-1} (1 - \tau^2)]^2 \}^{1/2} \sin \left(\frac{2\pi vt}{\Delta} + \varphi_0 \right).$$

§ 2. Layout and Construction of the Model

A block diagram of the model and circuit diagrams of its parts are shown in Fig. 1. In making the model we used commercial resistors and capacitors. The inductances and resistances of less than 10Ω were made by hand. For the resistances the deviation from nominal was not more than 2% and for the reactances, not more than 10%.

Conversion from mechanical to electrical quantities and vice versa was based on the data given in Table 1. The Young's modulus of the vessel wall was assumed to be $4 \cdot 10^5 \text{ kgf} \cdot \text{m}^{-2}$, the viscosity of the blood $3 \cdot 10^{-3} \text{ kgf} \cdot \text{m}^{-1} \cdot \text{sec}^{-1}$, and its density $1.05 \cdot 10^3 \text{ kgf} \cdot \text{m}^{-3}$. The radii of the segments, their lengths, and the values of the flow friction, the elasticity, and the inertia of the blood for these segments, together with the corresponding data for the pump, calculated from the expressions $R = 8\pi\mu l/F^2$; $C = 3Fr_W l/2Eh$; $L = \rho l/F$, are given in Table 2. The peripheral resistance of the organs was calculated starting from data on the mean rate of flow through the organ, and their elasticity was assumed, as in [2], to be proportional to

TABLE 1.

Quantity	Units	
	hydrodynamic	electrical
Time	1 sec	10^{-4} sec
Frequency	1 Hz	10^4 Hz
Capacity	1 m^3	10^{-2} C
Flow	$1 \text{ m}^3 \cdot \text{sec}^{-1}$	10^2 A
Pressure	$1 \text{ mm Hg} = 1.33 \cdot 10^2 \text{ kgf} \cdot \text{m}^{-1} \cdot \text{sec}^{-2}$	10^{-1} V
Resistance	$1 \text{ kgf} \cdot \text{m}^{-4} \cdot \text{sec}^{-1}$	$7.5 \cdot 10^{-6} \Omega$
Elasticity	$1 \text{ kgf}^{-1} \cdot \text{m}^4 \cdot \text{sec}^2$	1,33 F
Inertia	$1 \text{ kgf} \cdot \text{m}^{-4}$	$7.5 \cdot 10^{-10}$ g-force

TABLE 2

Vessel	$r_w \cdot 10^2 \text{ m}$	$l \cdot 10^2 \text{ m}$	$R \cdot 10^2 \text{ kg} \cdot \text{m}^{-4} \cdot \text{sec}^{-1}$	$L \cdot 10^6 \text{ kgf} \cdot \text{m}^{-4}$	$C \cdot 10^{-11} \text{ kgf}^{-1} \cdot \text{m}^4 \cdot \text{sec}^2$	
Ascending aorta	1,40	5,5	0,15	2,1	119,0	
Arch of aorta	1,00	4,0	0,25	1,1	52,0	
Thoracic aorta	0,75	20,0	4,10	10,1	149,0	
Abdominal aorta	1	0,62	5,3	2,80	4,7	20,0
2	0,59	5,3	2,80	5,3	18,0	
3	0,55	5,3	4,50	6,0	16,0	
Iliac artery	0,36	6,0	33,00	12,0	6,9	
Femoral artery	0,28	40,0	390,00	110,0	15,0	
Innominate artery	0,62	3,4	2,80	3,0	13,0	
Left brachiocephalic artery	0,40	11,0	47,00	21,0	12,0	
ACA	0,77	95,0	31,00	72,0	—	

the volume of blood in them, using a proportionality factor of $0.3 \text{ kgf} \cdot \text{m}^{-1} \cdot \text{sec}^{-2}$. An exception was made for the vessels of the brain, which are almost incapable of expanding under pressure. The elasticity of the organs, their hydraulic resistance, and the resistance of the portal veins are given in Table 3. In the case of the artificial circulation simulator we took into account the resistance of the oxygenator, supply tubes, and cannula.

§ 3. Results of Simulation

Simulation was carried out in two different regimes. The first (regime A) simulated the normal functioning of the circulatory system. In this case the generator signal was supplied to the ascending aorta (segment 1 in Fig. 1); the part of the valve was played by a semiconductor diode. In the second case (regime B) artificial circulation was simulated. The signal was supplied to be femoral artery (segment 8), the generator was connected to the ACA analog, and the model was modified as described above.

Impedance. We measured the dependence of the impedance on the frequency of the sinusoidal signal. The results for regime A are shown in Fig. 2 together with the results for the model described in [3] and the results of direct measurements in man [4] obtained by dividing the corresponding pressure harmonics by the flow-rate harmonics. Accordingly, there are direct measurements only for frequencies that are multiples of the pulse rate. It is clear from these graphs that the impedance measured on the proposed model is closer to the actual impedance than in the case of the more detailed model of [3]: in the latter the compliance of the organs was disregarded, so that the impedance oscillates more rapidly than in fact it should. The discrepancies between the actual impedance and the results of the simulation at high frequencies are evidently associated with the inertia and viscous properties of the vessel wall, which were not taken into account in the model. However, for the first and fundamental harmonics of the heart the model reproduces the actual impedance quite well.

The frequency dependence of the impedance for regime B is also shown in Fig. 2. The sharp increase in impedance is associated with the fact that the femoral artery is smaller and stiffer than the aorta.

The total flow friction in regime B is approximately twice as great as in regime A. This is due, firstly, to the introduction of additional resistances (oxygenator, cannula, increase in the resistance of the femoral artery owing to flow turbulence) and, secondly, to the functional modification of the model (signal supplied to the femoral artery).

TABLE 3

Organ, limb, vessel	$10^3 \text{ kgf} \cdot \text{m}^{-4} \cdot \text{sec}^{-1}$	$10^{-11} \text{ kgf}^{-1} \cdot \text{m}^4 \cdot \text{sec}^2$
Heart	24,00	6,8
Brain 1	20,00	—
2	20,00	100,0
Right arm	20,00	—
Left arm	23,00	100,0
Neck	45,00	84,0
Liver	18,40	21,0
Ventricle (spleen)	13,80	230,0
Intestine 1	7,70	150,0
2	37,50	60,0
Kidneys	6,10	100,0
Leg 1	42,80	60,0
2	19,60	260,0
Portal vein 1	0,12	—
2	0,40	—

Wave Propagation. For regime B the shapes of the pressure and flow waves in the ascending, thoracic, and abdominal aorta and in the femoral artery are shown in Fig. 3. Here it is possible to observe the effect, known in physiology, of a peripheral increase in pressure-wave amplitude and decrease in flow-wave amplitude. This effect was discussed in [3], where the increase in pressure amplitude was attributed to interference of the primary and reflected waves, and the decrease in flow-rate amplitude to ramification of the flow.

In regime B the pressure-wave amplitude fell sharply in the femoral artery as compared with the starting value produced by the pump, but in the aorta remained almost constant. The flow amplitude decreased with distance from the femoral artery, but the ratio of this amplitude to the mean flow rate actually increased. If it is recalled that in regime A this ratio decreased, then the considerations advanced by the authors of [3] are insufficient to explain the wave propagation in the model.

A possible explanation of the effects associated with wave propagation is the influence of the decrease in the radius of the aorta, which in the model was taken into account "in steps." In [5] flow in a slowly tapering vessel was investigated by the small-parameter method. The nature of the solution obtained by the authors makes it possible to attribute the model effects to the variation in the mean radius of the aorta from the heart toward the periphery.

CONCLUSIONS

1. By taking into account the elasticity of the vascular system of the internal organs it is possible to simulate the impedance with high accuracy on a quite simple model.
2. Perfusion through the femoral artery sharply increases the resistance and especially the reactance because of the changed distribution of the blood flow in the vascular system.
3. The change in the amplitudes of the pressure and flow pulse waves toward the periphery is primarily associated with the change in vessel geometry, not with wave reflection.
4. A whole series of factors, such as an increase in total impedance, the change in wave amplitude along the aorta, the almost total absence of high-frequency harmonics, leads to a decrease in pressure pulsation in the case of perfusion through the femoral artery. Clearly, the decrease in pulsation amplitude should, in its turn, affect the nonlinear component of the carotid sinus reflex.
5. Reversing the blood flow in the femoral artery and the aorta leads to a decrease in the mean arterial pressure (up to 10%) in the head and upper limbs as compared with the other parts of the body, which clearly can also have an unfavorable effect on the activity of the organism.

LITERATURE CITED

1. G. N. Jager, "Electrical model of the human systemic arterial tree," Thesis, University of Utrecht (1965).
2. M. F. Snyder, V. C. Rideout, and R. J. Hillestad, "Computer modeling of the human systemic arterial tree," *J. Biomech.*, 1, No. 4, 341-353 (1968).
3. N. Westerhof, F. Bosman, C. DeVries, and A. Noordergraf, "Analog studies of the human systemic arterial tree," *J. Biomech.*, 2, 121-143 (1969).
4. D. J. Patel, J. C. Greenfield Jr., and D. L. Fry, "In vivo pressure length radius relationship of certain blood vessels in man and dog," in: *Pulsatile Blood Flow*, New York (1964), pp. 293-302.
5. J. Mirsky, "Pulse velocities in cylindrical tapered and curved anisotropic elastic arteries," *Bull. Math. Biol.*, 35, 495-511 (1973).